CrystEngComm

Accepted Manuscript

ROYAL SOCIETY OF CHEMISTRY

www.rsc.org/crystengcomm

CrystEngComm

PAPER

Structural transition control between dipole−dipole and hydrogen bonds induced chirality and achirality

Received 00th January 20xx,
Accepted 00th January 20xx

DOI: 10.1039/x0xx00000x

www.rsc.org/

Yi Hu, Kai Miao, Shan Peng, Bao Zha, Li Xu,* Xinrui Miao and Wenli Deng*

Nano-fabrication is an issue gained extensive attention in molecular engineering. Thus we intensively probed surface-based 2D self-assembly of 2-hydroxyanthraquinone (2-HA) derivatives by scanning tunneling microscopy (STM). During the STM process, two interesting nanostructures extremely resembled Chinese knot and wheat, thus they were denoted as Knot-like and Wheat-like patterns for legibility. Moreover, careful observation suggests that the Knot-like structure is chiral while the Wheat-like structure is achiral. Systematic analysis indicates that these two arrangements are mainly dominated by synergistic forces of dipole−dipole and hydrogen bonding interactions. To the best of our knowledge, the dipole induced chirality and achirality has been rarely reported, and the synergistic forces of dipole−dipole and hydrogen bonding interactions on dominating 2D assembly have never been proposed. In addition, structural transition between the Knot-like and Wheat-like configurations can be regulated by concentration and solvent as the alkyl chain length changes. Note that the phase transformation is in most cases incomplete. A summary of surface coverage for 2-HA-OC_n (n = 12, 14, 16, 18, 20) molecules shows the general trend that Knot-like structure is preferred in polar solvent and under low concentration, while Wheat-like structure takes priority in nonpolar solvent and under high concentration. Besides, 2-HA-OC_n (n = 11, 13, 15, 17) molecules adopted Wheat-like′ pattern which differs from the Wheat-like pattern in the relative orientation of adjacent ribbons, ascribing to minimum of steric repulsion between the interdigitated alkyl chains. The study presents efficient strategies on manipulation of chiral and achiral nanostructures, and the results are believed to be of significance to the fields of 2D self-assembly and interface science.

1. Introduction

Exploring and controlling the 2D pattern formation of organic molecules on surface have attracted extensive attentions and been an active research area.[1-8] Chirality is a common phenomenon in nature, and surface chirality has gained wide-spread interest. Studies of the induction, transformation, and amplification of chirality provide fundamental understanding and potential applications on enantioselective catalysis, chiral separation and many other physical, chemical and biological topics.[9-14] The liquid/solid interface provides ideal environment to induce ordered 2D self-assembly adlayers by physisorption under dynamic and thermodynamic control.[15] To date, STM remains to be one of the preferred techniques for investigating the ordering of the monolayer, owing to its time-dependent observation and atomic resolution.[16] Therefore, probing the structure of the monolayer on solid surface by STM and tuning the arrangement of molecules by multiple factors such as temperature,[17,18] substrate,[19] functional groups,[20,21] scanning time,[22] nature of the solvent,[15,23-27] concentration of the solution,[1,28-32] are of great challenge and significance in 2D crystal engineering. Investigation of structural transition from chirality to achirality for achiral molecules on achiral substrate of highly oriented pyrolytic graphite (HOPG) is of great importance to the fields of assembly polymorphism and surface research, and Deng's group has reported this phenomenon.[31,33] They presented the solvent induced structure transition of 2-hydroxy-7-pentadecyloxy-9-fluorenone (HPF) molecules through co-assembly of achiral aliphatic solvent under the concentration which varied in an extensive range. The supramolecular nanostructures were constructed *via* van der Waals interactions between the solute and solvent molecules. Interestingly, the chiral pattern would finally change into achiral structure, which had been proved to be a dynamically stable configuration. Therefore, we believe that whether the self-assembled structure is chiral or achiral can be regulated. In another case, the co-adsorbed solvent molecules play an important role in manipulating the chirality through hydrogen bonds. For example, Wan *et al*. reported the induction of global homochirality in 2D enantiomorphous networks of achiral molecule of 5-(benzyloxy)-isophthalic acid derivative (BIC) *via* hydrogen bonding interaction with the chiral co-absorbers of 1-octanol and 2-octanol.[9] Another important factor reported to induce or affect the molecular chiral assembly is alkyl chain length. For instance, Li and his group have investigated the self-assembly of 1,7,13-trialkanoyldecacyclene derivatives of TTD (with alkyl chains of n= 14) and TOD (with alkyl chains of n = 18), respectively.[34] They found that the enantiomorphous domains of TTD were formed but no chiral domains were observed for TOD. Then we conclude that the

College of Materials Science and Engineering, South China University of Technology, Guangzhou 510640, China. E-mail: mslxu@scut.edu.cn, wldeng@scut.edu.cn; Tel: 86-20-22236708

† Electronic Supplementary Information (ESI) available: Detailed description of experimental section and additional STM images. See DOI: 10.1039/x0xx00000x

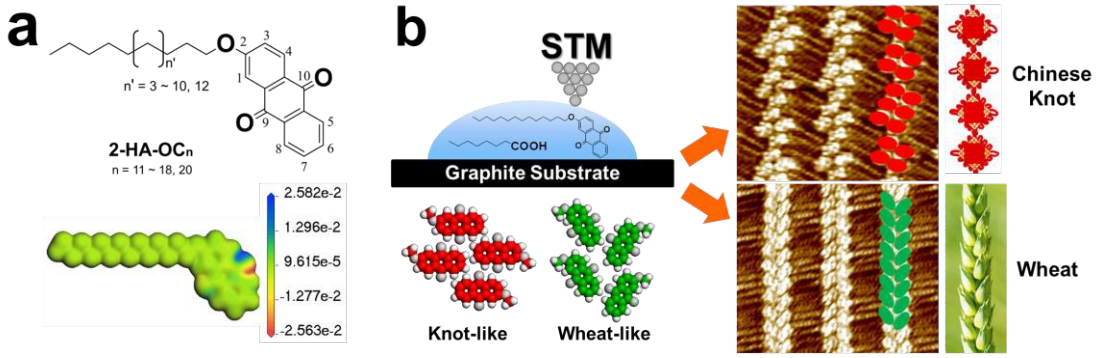

Fig. 1 (a) Chemical structure of 2-HA-OC_n and the calculated electrostatic potential map of 2-HA-OC_{14} using Material Studio 4.4. The 2-HA-OC_n molecules show polarity, and the direction of the dipole moment is from the positive part to the negative part. (b) Two basic structures named as Knot-like and Wheat-like, and the real pictures for Chinese knot and wheat[35] (used with modification).

chiral and achiral expressions are caused by cooperative interactions between the π-conjugated cores and the side chains, together with the effect of substrate.

On the whole, chirality and achirality can be manipulated by solvent, concentration and alkyl chain length *via* hydrogen bonds or van der Waals interactions. Nevertheless, the supramolecular chirality constructed dominantly *via* dipole−dipole interaction on achiral surface of HOPG has seldom been reported. So we explored the chiral and achiral nanostructures which are dominated by the synergistic forces of dipole−dipole and hydrogen bonding interactions, and lay emphasis on controlling the phase transition between chirality and achirality through changing the solvent and concentration.

Herein, we present systematic investigation of the 2D self-assembly of 2-hydroxyanthraquinone derivatives (named as 2-HA-OC_n, *n* = 11−18, 20) and strategies on regulation of the structural transformation. 2-HA-OC_n molecule shows polarity. The achiral and asymmetric 2-HA-OC_n molecule has a well-defined chemical structure which consists a π-conjugated anthraquinone core and an alkyl chain in the 2-position. Therefore, 2-HA-OC_n molecules self-assembled into a head-to-head fashion through dipole−dipole interactions. Besides, from the calculated electrostatic potential map of 2-HA-OC_{14} in Fig. 1a, it can be seen that the O atom in the 10-positon has both positive and negative electrostatic parts, but the O atom in the 9-position nearly does not. As a result, from the viewpoint of electrostatic interaction, the 2-HA-OC_n molecules also tend to be doubly bonded. During the process of our STM experiment, two interesting structures were observed. One resembles the traditional Chinese knot which originates from the Old Stone Age (around 8,000 B. C.). The other resembles the world-distributed crop of wheat. Therefore, the two self-assembled arrangements investigated by STM are named as Knot-like and Wheat-like structures for novelty and ease to be discerned. We found that the surface coverage for these two phases could be regulated. As the solvent polarity decreased, surface coverage of the Knot-like structure correspondingly decreased. Thus we confirm that the chiral structure of Knot-like is favored in polar solvent, whereas the achiral structure of Wheat-like is preferred in nonpolar solvent. Besides, when *n*-tetradecane was used, the surface coverage of Knot-like structure increased as the alkyl chain length increased, indicating that alkyl chain length played an important role in affecting the 2D self-assembly. Concentration also showed great regulation on these two phases. Wheat-like arrangement was preferred at high concentration, while Knot-like configuration was the main structure at low concentration. In addition, odd−even effect was a usual phenomenon. 2-HA-OC_{odd} molecules self-assembled into ordered monolayer named as Wheat-like′, which differed from the Wheat-like structure of 2-HA-OC_{even} in the relative orientation of adjacent rows. On the whole, we systematically explored the surface distribution of chirality and achirality, thus the results can better promote our understanding of dipole and hydrogen bonds induced chiral and achiral expressions and provide us strategies for efficient fabrication and regulation of molecular monolayers.

2. Experimental Section

2-Hydroxyanthraquinone derivatives (2-HA-OC_n, *n* = 11−18, 20) were synthesized using a method we have described previously[36], and the characterization data confirming the structures and purity of the compounds are described in the supporting information (Scheme S1†). The solvents of 1-octanoic acid, 1-phenyloctane, and *n*-tetradecane were purchased from TCI and used without further purification. The 100% saturated solutions (concentration: C_0) were prepared at first, then diluted to 50% saturated (1/2 C_0) and 10% saturated (1/10 C_0). The values of concentration for 100% saturated solutions of 2-HA-OC_n molecules are shown in Table S1(†). The samples were prepared by depositing a droplet (about 1μL) of solution onto a freshly cleaved atomically flat surface of HOPG (quality ZYB, Bruker, USA). STM experiments were performed on a Nanoscope IIIa Multimode SPM (Bruker, USA) under ambient condition (temperature: 15−20°C, humidity: 45−60%). The tips were mechanically cut from Pt/In wires (80/20). Different tips and samples were used to check the reproducibility of the results. All images were recorded with constant current mode and shown without further processing. Imaging conditions are given in the corresponding figure captions. Material studio 4.4 was used to build molecular models of the assembled structures. The models were constructed based on the inter-molecular distances and angles, and analysis of the STM results. Also, they were tested to be right

according to the ideal overlap with the high-resolution STM images. The surface coverage and the corresponding error in this work are calculated with methods as described in the supporting information. Note that the area percentage given in the paper is an average value of several large-scale (100 × 100 nm^2) images. The DSC experiments were conducted with a scan rate of 10 °C min^{-1} for heating and cooling traces (instrument information: NETZSCH DSC 200F3).

3. Results

3.1 Knot-like and Wheat-like structures for 2-HA-OC_{14} at the 1-octanoic acid/HOPG interface (concentration: 50% saturation)

First of all, we investigated the self-assembly configurations of 2-HA-OC_{14} (Fig. 2a) at the liquid/HOPG interface. Fig. 2b is the large-scale STM image for 2-HA-OC_{14} molecules physisorbed on HOPG surface, with 1-octanoic acid as the solvent and under the concentration of 50% saturation (4.8 × 10^{-3} mol L^{-1}). It is clear that the monolayer consists of two domains, which are termed as Knot-like and Wheat-like structures and marked as I and II (Fig. 2b), respectively. The shape of 2-HA-OC_{14} molecules can be identified by the HOMO level, as shown in Fig. 2a. The anthraquinone cores appear as bright spots due to the highly delocalized electrons, whereas the less bright lines are attributed to the side chains. Fig. 2c and 2e are the high-resolution STM images, showing the structural details of domain I and II.

In Fig. 2c, every four or six molecules gather together in a head-to-head mode, as denoted by four red ovals and six green ovals, respectively. Careful observation suggests that the emergences for these tetramers and hexamers are not disciplinary. In a ribbon, the neighbors of a tetramer are two hexamers, or two tetramers, or a hexamer and a tetramer. However, in adjacent ribbons, these irregularly emerged tetramers and hexamers are staggered in a perfectly dense packing fashion, and the alkyl chains are fully interdigitated. Molecules in the polymers are arranged with every two head-to-head anthraquinone units antiparallel to each other. A set of black arrows in the left bottom of Fig. 2c show the 3-fold symmetry of the underlying HOPG substrate. The side chains show good commensurability with the graphite surface and extend along one of the main symmetry axes of HOPG in order to maximize the adsorbate−substrate interaction. On the basis of STM results, a structural model for this Knot-like structure is proposed in Fig. 2d. The unit cell is superimposed on the image with parameters of a = 5.5 ± 0.2 nm, b = 3.6 ± 0.2 nm and α = 67 ± 2°, which are consistent with the STM measurements. Every unit cell consists of ten molecules and the calculated area density is 1.82 nm^2 per molecule.

In domain II, 2-HA-OC_{14} molecules are densely arranged with each other in a head-to-head fashion, leading to orderly ribbons which are constituted from double rows of bright spots, as shown in the high-resolution STM image of Fig. 2e. Interestingly, the two rows of molecules in a ribbon stagger in a V-like style, which is obviously different from the antiparallel one in the Knot-like structure. The main symmetry axes of the HOPG surface are illustrated by six black arrows in Fig. 2e. Alkyl chains in this Wheat-like configuration are fully interdigitated, extending along one of the main directions of the graphite lattice. As a result, molecules are firmly adsorbed on the graphite surface through chain−chain and chain−substrate van der Waals interactions. Close examination of the image in Fig. 2e reveals that the adjacent ribbons are reverse to each other, with the V-like shapes orienting to opposite direction, as denoted by blue and red arrows for legibility. According to the STM results, a structural model is proposed in Fig. 3f. A unit cell composed of four molecules is overlaid with the measured unit cell parameters of a = 0.9 ± 0.1 nm, b = 6.3 ± 0.1 nm, α = 84 ± 1°, and the calculated area density is 1.41 nm^2 per molecule.

The 2-HA-OC_{14} molecules show polarity, and consequently, they are doubly bonded into head-to-head fashion *via*

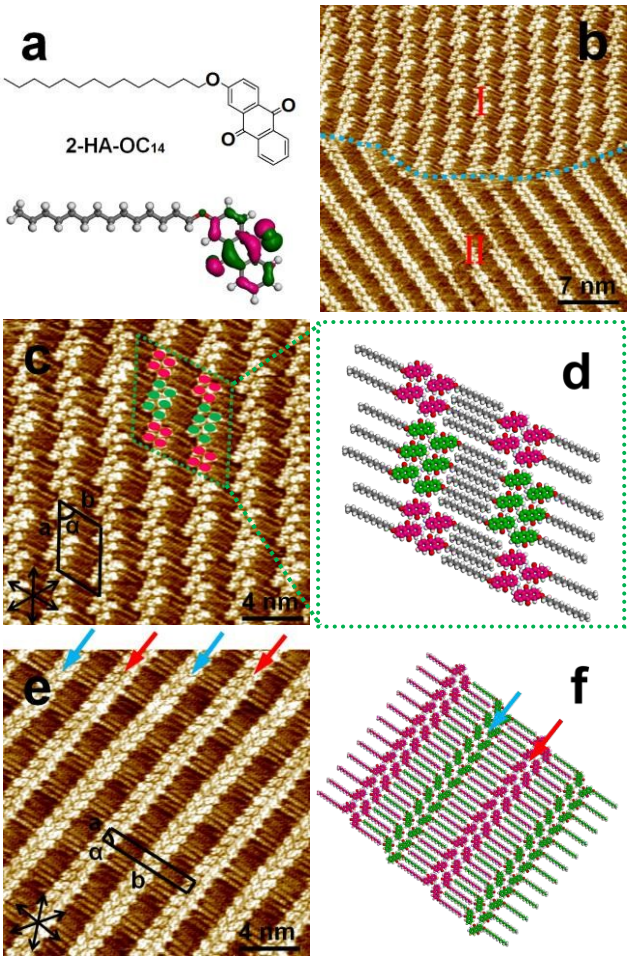

Fig. 2 (a) Chemical structure of 2-HA-OC_{14} molecule and the calculated charge density contours of HOMO using Material Studio 4.4. (b) Large-scale STM image for 2-HA-OC_{14} physisorbed on 1-octanoic acid/HOPG surface under the concentration of 50% saturation (4.8 × 10^{-3} mol L^{-1}). (c and e) High-resolution STM images for Knot-like and Wheat-like structures. A set of black arrows indicate the direction of the main symmetry axes of the graphite. The tetramer and hexamer are marked in (c) by four red and six green ovals, respectively. Adjacent ribbons with reverse direction are distinguished by red and blue arrows in (e). (d and f) The proposed molecular models for Knot-like and Wheat-like structures. Imaging condition: I_t = 400−710 pA, V_{bias} = 550−800 mV.

dipole−dipole interactions, forming these Knot-like and Wheat-like patterns. In addition, weak C=O···H-C hydrogen bonds act a significant role in forming these two patterns, with the carbonyl oxygen as an acceptor and hydrogen in the adjacent anthraquinone moieties as a donor. Therefore, these two configurations are dominated and stabilized by the synergistic forces of dipole−dipole and hydrogen bonding interactions. However, packing densities for these two assembly arrangements are obviously different. Compared with the Knot-like structure, the average surface area of a single molecule is smaller for Wheat-like structure, namely, the latter is denser than the former. For the sake of exploring the stability of the two patterns, the sample was characterized for three hours without cease. As a result, we found that the two structures were stably coexistent because no transformation between the Knot-like and Wheat-like phases could be found.

3.2 Chiral structure for 2-HA-OC_{16} at the 1-octanoic acid/HOPG interface (concentration: 50% saturation)

With further research, we increased the alkyl chain length to n = 16. When 1-octanoic acid was used as the solvent under the concentration of 50% saturation (4.5 × 10^{-3} mol L^{-1}), only Knot-like structure was observed in a large-scale STM image (Fig. S2†). Although different samples with the same concentration were probed at different places, no Wheat-like structure was found. Fig. 3a shows a representative STM image with clear and well-defined pattern. When molecules adsorbed onto the surface, two chiral adsorption conformations with mirror symmetry instantaneously formed in enantiomer domains, which are separated by blue dotted lines. The rotation directions of clockwise (CW) and counter clockwise (CCW) are denoted by blue and green open-circle arrows, respectively. The high-resolution STM images showed in Fig. 3b and 3c manifest more structural details. Similarly with the Knot-like structure for 2-HA-OC_{14}, tetramers and hexamers are the basic units of the adlayer. The polar 2-HA-OC_n molecule tends to arrange in a head-to-head fashion *via* dipole−dipole interaction. Six or four 2-HA-OC_{16} molecules in turn form the enantiotopic multimer structure according to the direction of the dipole moments, as marked by blue arrows in Fig. 3d. We identify the multimer structure as CW and CCW. On the basis of symmetry and intermolecular distance, basic unit cells are superimposed in Fig. 3b and 3c, with parameters of a = 4.6 ± 0.2 nm, b = 3.7 ± 0.2 nm, α = 73 ± 1° for CCW configuration, and a = 4.6 ± 0.2 nm, b = 3.8 ± 0.2 nm, α= 73 ± 1° for CW configuration. The molecular density is about 1.63 nm^2 per molecule. For the sake of clarity, structural models for the chiral conformations are proposed in Fig. 3e and 3f. This phenomenon of chirality can also be observed for the Knot-like structure of 2-HA-OC_{14} molecules. As the adlayer consists of coexistent Knot-like and Wheat-like structures, chiral domains with good consecutiveness were usually separated by Wheat-like structure (Fig. S3†).

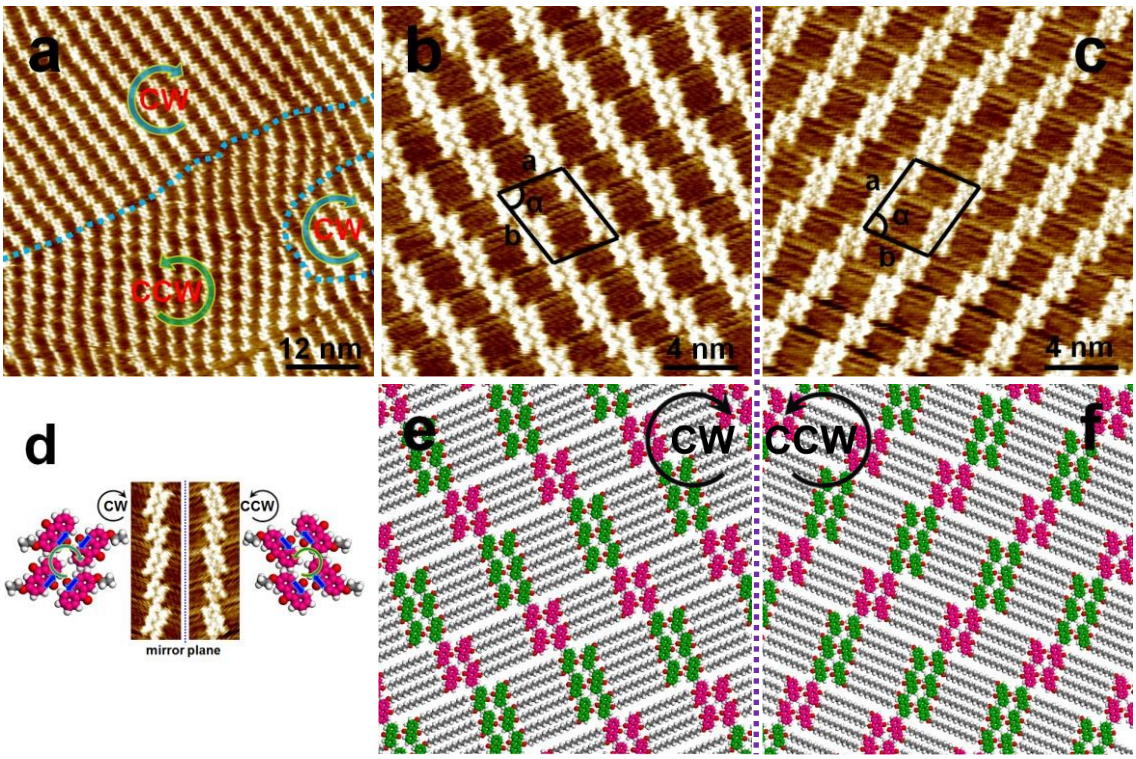

Fig. 3 (a) Large-scale STM image of 2-HA-OC_{16} molecules self-assembled monolayer at 1-octanoic acid/HOPG interface under the concentration of 50% saturation (4.5 × 10^{-3} mol L^{-1}). The blue and green open-circle arrows indicate the CW and CCW patterns. (b and c) High-resolution STM images for the chiral patterns of CW and CCW. (d) Magnified images of the basic mirror tetramers and hexamers. The blue arrows indicate the dipole direction of the 2-HA-OC_{16} molecules. (e and f) The proposed structural models for CW and CCW structures. Imaging condition: I_t = 450−710 pA, V_{bias} = 500−850 mV.

3.3 Chiral and achiral patterns for 2-HA-OC_{even} (n = 12, 18, 20) at the 1-octanoic acid/HOPG interface (concentration: 50% saturation)

Under the concentration of 50% saturation in 1-octanoic acid, 2-HA-OC_{14} and 2-HA-OC_{16} showed different self-assembly tendency to form Wheat-like and Knot-like structures. To further explore how surface coverage could be regulated as the alkyl chain length changed, we synthesized other 2-HA-OC_n derivatives by decreasing the alkyl chain length to n = 12 and increasing the alkyl chain length to n = 18 and 20.

In the condition of the same solvent and concentration with 2-HA-$OC_{14,16}$, the large-scale STM image (see Fig. 4a) of 2-HA-OC_{12} shows that only Wheat-like configuration are observed. Knot-like structure was not found even though we scanned the sample repeatedly and scanned in different places. The structural details are revealed by a high-resolution STM image shown in Fig. 4d. A unit cell is outlined with a = 0.8 ± 0.3 nm, b = 5.9 ± 0.3 nm and α = 89 ± 2°. The calculated area density is 1.18 nm^2 per molecule. Then a question arises: as the alkyl chain length gradually decreased from n = 16 to 14 to 12, why the assembled structures correspondingly transferred from Knot-like to Wheat-like. According to the calculated area density for these two structures of 2-HA-OC_{14}, we have proved that the Knot-like phase is looser than Wheat-like phase. The 2D self-assembly configuration at the liquid/solid interface involves a balance and competition between adsorption and desorption of the solute molecules.[24] As the alkyl chain length decreases, van der Waals interaction between solvent and solute molecules decreases. Therefore, in unit time, the number of molecules adsorbed from the solution onto the graphite surface within the unit area increases, and consequently favors the denser Wheat-like arrangement.

However, as the alkyl chain length increased to n = 18, the Wheat-like structure appeared again, instead of only Knot-like structure as in the case of n = 16. From the large-scale STM image shown in Fig. 4b, it can be clearly seen that the monolayer consists of both CW and CCW Knot-like fashions, and the chiral domains are separated by Wheat-like domains which occur randomly. There's no difference between the adlayers of 2-HA-OC_{14} and 2-HA-OC_{18}, except for the basic unit cells which are superimposed in the high-resolution STM images (Fig. 4e and 4f). The parameters are measured to be a = 4.9 ± 0.1 nm, b = 4.2 ± 0.1 nm, α = 78 ± 2° for Knot-like pattern and a = 0.9 ± 0.2 nm, b = 8.6 ± 0.2 nm, α = 88 ± 1° for Wheat-like pattern. When the alkyl chain is further longer (n = 20), we found that the substrate was also covered with coexistent Wheat-like and Knot-like structures, and chirality could be easily observed, as indicated in Fig. 4c. The high-resolution STM image which manifests more details for 2-HA-OC_{20} is shown in supporting information (Fig. S4†). This is an interesting phenomenon because

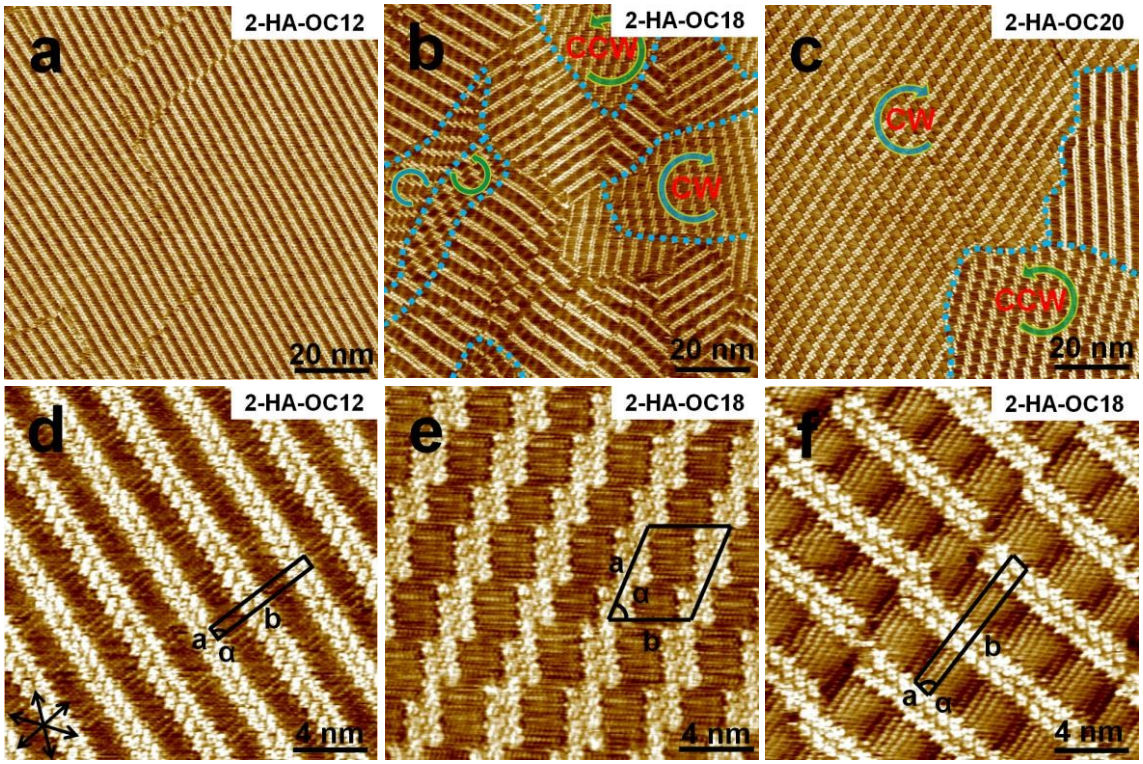

Fig. 4 (a–c) Large-scale STM image of 2-HA-OC_{12}, 2-HA-OC_{18} and 2-HA-OC_{20} molecules self-assembled monolayers at 1-octanoic acid/HOPG interface under the concentration of 50% saturation (5.5×10^{-3}, 2.1×10^{-3}, 1.9×10^{-3} mol L^{-1} for n = 12, 18, 20). The chiral patterns of CW and CCW in (b) and (c) are denoted by blue and green open-circle arrows, according to the dipole direction of the 2-HA-OC_n molecules. (d) High-resolution STM image for 2-HA-OC_{12}, showing the Wheat-like structure. (e and f) High-resolution STM images of 2-HA-OC_{18} molecules, indicating the Knot-like and Wheat-like configurations, respectively. Imaging condition: I_t = 400–730 pA, V_{bias} = 450–850 mV.

Table 1. Surface coverage (%) of Knot-like and Wheat-like patterns in 1-octanoic acid under different concentration for 2-HA-OC_n molecules.

	n	12	14	16	18	20
50% saturation	Knot-like	0	49.7	99.5	72.1	82.8
	Wheat-like	99.5	50.1	0	27.7	17.0
10% saturation	Knot-like	0	74.6	99.7	97.8	90.5
	Wheat-like	99.7	25.2	0	2.0	9.2
100% saturation	Knot-like	0	40.2	99.4	28.9	34.4
	Wheat-like	99.8	59.6	0	70.9	65.5

the structural variation tendency for the circumstance of $n > 16$ is completely different from that for the circumstance of $n < 16$. As the alkyl chain length increases, the molecule−molecule and molecule−substrate interactions increase at the same time, so the denser pattern shows possibility. Consequently, the appearance of densely packed Wheat-like pattern in the monolayer is absolutely possible.

3.4 Surface coverage control between chirality and achirality by changing the concentration (solvent: 1-octanoic acid)

We found that the ratio of the two polymorphs can be controlled by adjusting the 2-HA-OC_n concentration. The surface coverage of Knot-like and Wheat-like patterns in 1-octanoic acid under the concentration of 50% saturation are calculated, as summarized in the 2nd and 3rd lines in Table 1. The surface overage of self-assembled structures cannot reach 100% because of the emergence of monolayer defects.

To modulate the surface coverage, we firstly decreased the solution concentration to 10% saturation by diluting the 100% saturated solution with accurate proportion. No Knot-like structure was observed for 2-HAOC_{12}, that is to say, the Wheat-like structure was stable under low concentration. But for 2-HA-OC_{14}, an obvious structural transition was found, as shown in Fig. 5. Separated domains of Knot-like and Wheat-like structures were formed spontaneously as a drop of solution was deposited onto the graphite surface (Fig. 5a). When the same area was scanned repeatedly, the Knot-like domain gradually enlarged, but the whole surface was not covered by Knot-like structure totally. As shown in Fig. 5b, three minutes later, the growth for Knot-like domain stopped. The average surface coverage is 74.6% for Knot-like structure and 25.2% for Wheat-like structure, based on analysis of more than ten large-scale images (100 × 100 nm^2). Interestingly, under the low concentration of 10% saturation, Wheat-like configuration was barely or seldom to be found for 2-HA-$OC_{16,18,20}$ molecules. Also, no structural transition happened. The HOPG surface is mainly covered by Knot-like structure, and the surface coverage of Knot-like and Wheat-like patterns are summarized in the fourth and fifth lines of Table 1.

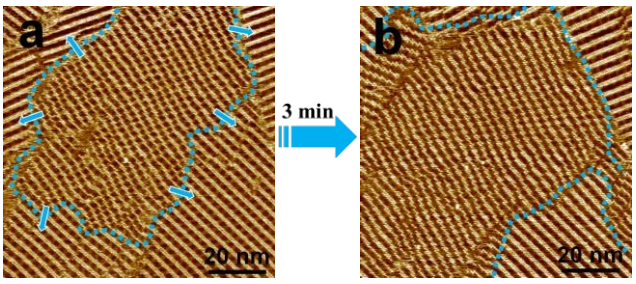

Fig. 5 Large-scale STM images for 2-HA-OC_{14}, depicting the instantaneous phase transition from Wheat-like to Knot-like pattern in 1-octanoic acid under low concentration of 10% saturation (9.5 × 10^{-4} mol L^{-1}). The Knot-like domain in (a) stopped to enlarge three minutes later. Imaging condition: I_t = 510 pA, V_{bias} = 650 mV.

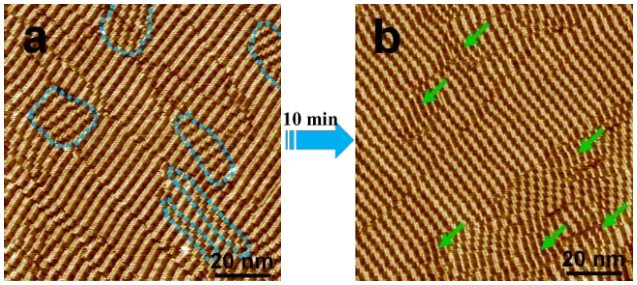

Fig. 6 Large-scale STM images for 2-HA-OC_{16}, depicting the phase transition from Wheat-like to Knot-like pattern in 100% saturated 1-octanoic acid. The Knot-like domain in (a) is seldom to be found, and ten minutes later the whole surface is covered by Knot-like structure (b). Monolayer defects are indicated by green arrows. Imaging condition: I_t = 560 pA, V_{bias} = 600 mV.

To gain further insight into the concentration effect on the self-assembly of 2-HA-OC_n molecules, the 100% saturated solutions were probed. Wheat-like structure was still the only configuration in the monolayer of 2-HA-OC_{12}. 2-HA-OC_{14} showed coexistent Knot-like and Wheat-like patterns and the surface coverage for them are 40.2% and 59.6%, respectively. For 2-HA-OC_{16}, structural transformation from Wheat-like pattern to Knot-like pattern was observed within ten minutes, as shown in Fig. 6. At first, apart from some small domains for Knot-like structure, as indicated by a series of blue dotted circles in Fig. 6a, the substrate was mainly covered by Wheat-like structure. However, ten minutes later, the HOPG surface was covered by Knot-like structure, except for some monolayer defects, which are marked by green arrows in Fig. 6b. The surface coverage for Knot-like configuration is 99.4%. Then we confirm that the Knot-like structure is the only stable structure for 2-HA-OC_{16} in 1-octanoic acid under any concentration. In addition, as the alkyl chain length increased to n = 18 and 20, Wheat-like structure appeared again. The two polymorphs were stably coexistent. For 2-HA-OC_{18}, the surface coverage ratios of Knot-like and Wheat-like structures are summarized in the last two lines of Table 1.

3.5 Surface coverage control between chirality and achirality by changing the solvent (concentration: 50% saturation)

In our study, solvent molecules did not play a counterpart role in the assembly process, but the surface coverage for Knot-like and

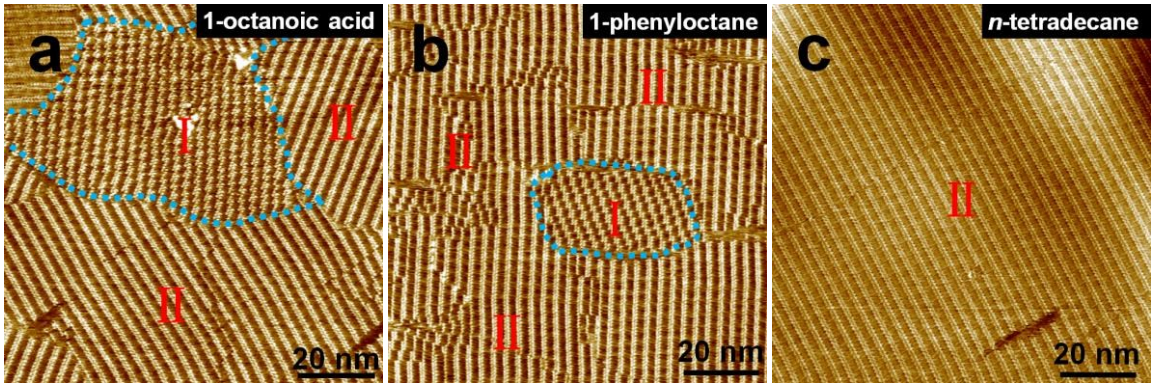

Fig. 7 Large-scale STM image of 2-HA-OC_{14} molecules self-assembled monolayers on HOPG surface in the solvents of 1-octanoic acid (a), 1-phenyloctane (b), and *n*-tetradecane (c) under the concentration of 50% saturation. Concentration: 4.8×10^{-3} mol L^{-1} for (a), 7.1×10^{-3} mol L^{-1} for (b), 1.1×10^{-6} mol L^{-1} for (c). Imaging condition: I_t = 510−780 pA, V_{bias} = 500−880 mV.

Wheat-like structures could be controlled by changing the solvent. A rich selection of solvent is needed for broadening our understanding of the solvent effect. So we choose three representative solvents of 1-octanoic acid, 1-phenyloctane and *n*-tetradecane, which differ from each other in their polarity. Even though 1-phenyloctane is classified into nonpolar group, it shows weak polarity falls in between 1-octanoic acid and *n*-tetradecane.[37] For 2-HA-OC_{14}, we found that under the concentration of 50% saturation, both of Knot-like and Wheat-like structures were favored in polar solvent of 1-octanoic acid (Fig. 7a), while in nonpolar solvent of *n*-tetradecane, only Wheat-like structure were observed (Fig. 7c). When 1-phenyloctane was used, we scanned the sample in different places and only a small domain of Knot-like structure was found (Fig. 7b). For the sake of further exploring how *n*-tetradecane can regulate the ratio of the two polymorphs, we systematically probed the self-assembly structures of 2-HA-$OC_{16,18,20}$ in 50% saturated solution (Fig. S5†). Interestingly, surface coverage for Knot-like structure gradually increased from 0% to 5.0%, 17.2% and 89.7% as the alkyl chain length increased from *n* = 14, to 16, 18 and 20. For ease of comparison, the detailed distributions for these two phases in polar and nonpolar solvents are shown in Fig. 8, and the surface coverage data are shown in Table S2 (†) and S3 (†).

Apart from 2-HA-OC_{12} molecules which only self-assembled into Wheat-like structure, both of the Knot-like and Wheat-like patterns for 2-HA-OC_n (n = 14, 16, 18, 20) can be obtained by changing the solvent and (or) concentration. In the histogram in Fig. 8a, the Knot-like structure takes a larger proportion, as the green section indicated. While in the histogram in Fig. 8b, the red section shows that the Wheat-like structure occupies a larger proportion. Then we conclude that the looser packed Knot-like pattern is favored in polar solvent, whereas the denser packed Wheat-like pattern is favored in nonpolar solvent. This is reasonable since *n*-tetradecane has low polarity, and thus has relatively weak interaction with the polar molecules of 2-HA-OC_n. As for 1-octanoic acid, stronger interaction exists between the solvent and solute because of its higher polarity. Moreover, there is a subtle balance and competition between adsorption and desorption of the solute molecules. Therefore, in a poor solvent of *n*-tetradecane, the solvophobic effect favors the adsorption of molecules at the liquid/solid interface thus a densely packed Wheat-like structure is more favored. On the other hand, in a good solvent of 1-octanoic acid, the solvophilic effect will increase the desorption rate at the liquid/solid interface, thus favoring Knot-like structure with low surface density.

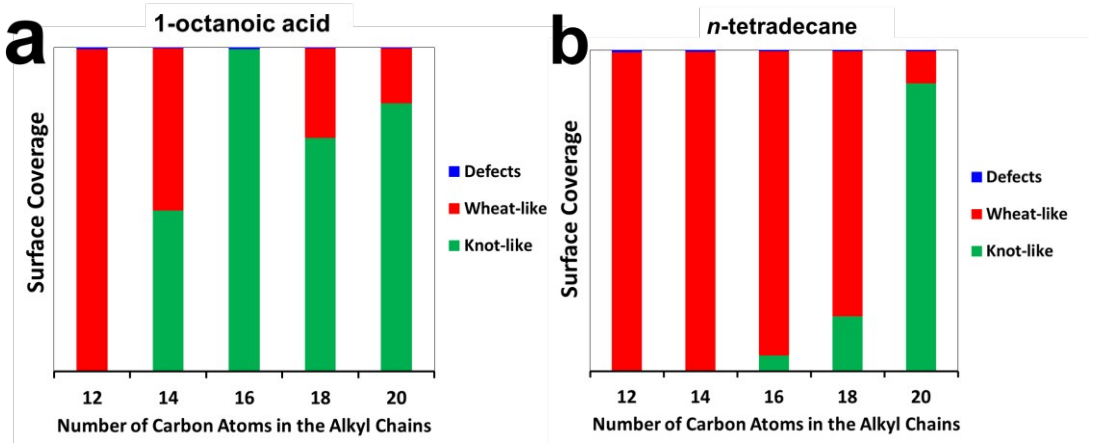

Fig. 8 Surface coverage distribution histograms for Knot-like and Wheat-like phases in polar and nonpolar solvents of 1-octanoic acid (a) and *n*-tetradecane (b).

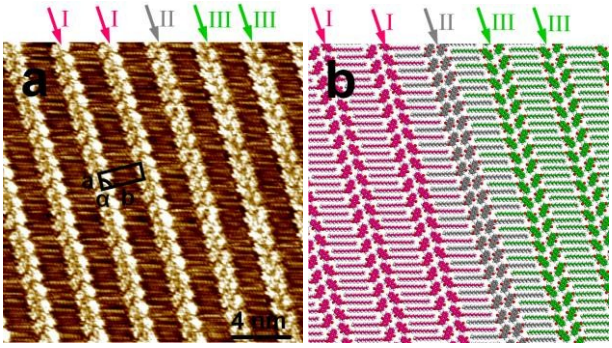

Fig. 9 (a) High-resolution STM image and (b) proposed molecular models for 2-HA-OC_{15}, showing the Wheat-like´ structure. Ribbon I, II and III are marked by arrows in different colors. Imaging condition: I_t = 550 pA, V_{bias} = 800 mV.

3.6 Self-assembly of 2-HA-OC_{odd} (*n* = 11, 13, 15, 17) at the 1-octanoic acid/HOPG interface (concentration: 50% saturation)

We have already systematically displayed how solvent and concentration could regulate the self-assembled adlayers of 2-HA-OC_n molecules with even-length alkyl chains. As a step further, we also explored the self-assembly patterns of 2-HA-OC_{11}, 2-HA-OC_{13}, 2-HA-OC_{15} and 2-HA-OC_{17}, and odd–even effect was found in the STM experiment process. Fig. 9a is the high-resolution STM image of 2-HA-OC_{15} molecules self-assembled monolayers at 1-octanoic acid/HOPG interface under the concentration of 50% saturation (4.6×10^{-3} mol L^{-1}). Molecules in a ribbon are arranged in a head-to-head fashion, and adjacent ribbons are densely packed through alkyl chain interdigitation. This structure is named as Wheat-like´. Careful observation suggests that there are three kinds of ribbons, which are defined as ribbon I, II and III, as indicated in Fig. 9a in different colors. Ribbon I and III are the same in their appearance, but different in their orientation. They direct to reverse direction. Differing from the V-like ribbon I and III, two rows of molecules in ribbon II are antiparallel to each other. The monolayer of 2-HA-OC_{15} can be considered as a combination of two domains: one domain constituted from ribbon I and the other constituted from ribbon III. Ribbon II is a perfect transition between these two domains, avoiding the occurrence of unstable domain boundary. The proposed molecular model for this structure is depicted in Fig. 9b, and different ribbons are modeled in different colors for ease of comparison and distinguishing. On the basis of symmetry and intermolecular distance, a basic unit cell is superimposed in Fig. 9a with parameters of a = 1.1 ± 0.3 nm, b = 3.0 ± 0.3 nm and α = 88 ± 1°. Every unit cell consists of two molecules and the calculated area density is 1.65 nm^2 per molecule. Besides, 2-HA-OC_{11}, 2-HA-OC_{13} and 2-HA-OC_{17} molecules self-assembled into the same configurations with 2-HA-OC_{15}, as indicated in the large-scale STM images in supporting information (Fig. S6†).

This Wheat-like´ configuration is unlike the Wheat-like structure for 2-HA-OC_n (*n* = even number). Adjacent ribbons in Wheat-like´ pattern point to the same direction, while in the Wheat-like structure, neighboring ribbons direct to opposite orientation. Odd-even effect is proposed as a result of the requirement for the end methyl group to minimize the steric repulsion.[38] Therefore, carbon atoms in adjacent chains should be staggered with each “up” atom in one chain next to a “down” atom in each of its neighbors. This will result in dense packing on surface, thus lowering the total potential energy of the system. The structural difference between Wheat-like configuration for molecules with even-length alkyl chains and Wheat-like´ configuration for molecules with odd-length alkyl chains originates from the difference of end methyl direction, and can be attributed to odd–even effect.

4. Discussion

Table 2 summarizes the geometric characteristics, unit cell parameters and packing density of the physisorbed adlayers of 2-HA-OC_n molecules at the 1-octanoic acid/HOPG interface.

Table 2. Schematic unit cell parameters and other characteristic parameters of the different structures observed in 2D self-assembly monolayers in 1-octanoic acid.

molecule	structure	*a* (nm)	*b* (nm)	*α* (°)	*N*	*S* (nm^2)	S_m (nm^2)
2-HA-OC_{12}	Wheat-like	0.8 ± 0.3	5.9 ± 0.3	89 ± 2	4	4.7	1.18
2-HA-OC_{14}	Knot-like*	5.5 ± 0.2	3.6 ± 0.2	67 ± 2	10	18.2	1.82
	Wheat-like	0.9 ± 0.1	6.3 ± 0.1	84 ± 1	4	5.64	1.41
2-HA-OC_{15}	Wheat-like´	1.1 ± 0.3	3.0 ± 0.3	88 ± 1	2	3.3	1.65
2-HA-OC_{16}	Knot-like*	4.6 ± 0.2	3.7 ± 0.2	73 ± 1	10	16.3	1.63
2-HA-OC_{18}	Knot-like*	4.9 ± 0.1	4.2 ± 0.1	78 ± 2	10	20.1	2.01
	Wheat-like	0.9 ± 0.2	8.6 ± 0.2	88 ± 1	4	7.7	1.93
2-HA-OC_{20}	Knot-like*	5.1 ± 0.3	4.5 ± 0.3	79 ± 1	10	22.5	2.25
	Wheat-like	0.9 ± 0.1	9.2 ± 0.1	87 ± 2	4	8.3	2.07

N = number of molecules per unit cell. *S* = unit cell area (nm^2). S_m = unit cell area divided by number of molecules per unit cell area. * Unit cell parameters are determined with the CCW patterns.

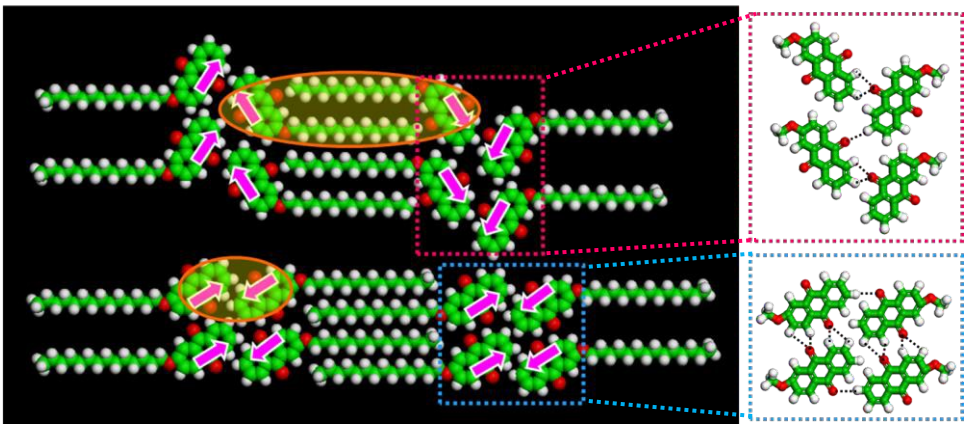

Fig. 10 Schematic diagrams with dipole alignments for Wheat-like (a) and Knot-like (b) structures. The dipole directions in these two patterns are depicted by pink arrows and the paired anthraquinone cores are denoted by orange ovals. The C-H···O=C hydrogen bonds for Wheat-like and Knot-like structures are enlarged in the red and blue dotted rectangles, respectively.

4.1 Dipole–dipole and hydrogen bonding interactions dominated chiral and achiral structures

The molecule–molecule, molecule–substrate, π–π stacking and electrostatic interactions are generally existent. Apart from them, the synergistic dipole–dipole and hydrogen bonding interactions play important roles in dominating the 2D self-assembly structures. The 2-HA-OC_n molecule shows polarity and it has an asymmetric chemical structure with an electron-rich anthraquinone core and an electron-poor alkyl chain. Weak dipolar interactions have been widely reported on controlling molecular placement and multicomponent monolayers.[39,40] In general, the molecular dipoles have the tendency of arranging in collinear or antiparallel modes to maximize the dipolar–dipolar interactions.[41] Close inspection of Wheat-like and Knot-like structure reveals that two rows of molecules in their basic ribbons take different arrangement fashions, means, V-like fashion for the former (Fig. 10a) and antiparallel fashion for the latter (Fig. 10b), respectively. The dipole directions in these two patterns are depicted by pink arrows. Every two anthraquinone cores align in an antiparallel way, as denoted by orange ovals, and form dipole pairs, which are viewed as stabilized state. It needs to explain that in Fig. 10a, the paired molecules come from two neighboring ribbons, thus the partners for the molecules in the edges are not depicted (the detailed information for the dipole direction of the lattice are shown in Fig. S7†). From the viewpoint of energy, polar molecules tend to arrange in a way that minimizes the overall polarity.[33] Therefore, these paired arrangements induced by dipole–dipole interactions are essential to avoid potential dipole repulsion[42], and consequently extinguish dipole moment around the self-assembled area to zero.

However, except for dipole–dipole interaction, van der Waals interaction between the alkyl chains also plays a significant role on regulating the 2D molecular structures. 2-HA-OC_{15} self-assembles into Wheat-like´ configuration, in which adjacent ribbons orient to the same direction (Fig. 9), thus no antiparallel pairs form to reduce the polarity of single molecule (see Fig. S8†). This is attributed to the competition of dipole–dipole interactions between the anthraquinone cores versus van der Waals interactions between the side chains, and the latter ones play the dominant role.

Weak hydrogen bonds can direct the formation of 2D crystalline structures because of their high directionality[43], and thus can regulate the molecular recognition process[44]. Hydrogen atom in the benzene ring has the ability to form C-H···O=C hydrogen bonds.[45,46] This weak interaction exists between the anthraquinone units have been reported by Tamaki *et al.*[47] to drive ordered 2D nanostructures. In this study, weak hydrogen bonding and dipole–dipole interactions are synergistic forces. The enlarged figures in the red and blue dotted rectangles in Fig. 10 are the illustration of C-H···O=C hydrogen bonds for Wheat-like and Knot-like structures between the anthraquinone units.

4.2 Controllable surface coverage of chiral and achiral patterns

Surface coverage of the Knot-like and Wheat-like phases can be modulated by changing the solvent polarity and solution concentration. Structural transition between the chiral Knot-like and achiral Wheat-like configurations is controllable. However, it should be pointed out that the structural transition is sometimes complete and sometimes incomplete.

4.2.1 Concentration control

As we know, self-assembly process at the liquid/solid interface is dynamic and depends on the adsorption–desorption equilibrium of the solute molecules.[48] In our present work, it is found that the relative occurrence for Knot-like and Wheat-like structures changes as the solution concentration varies from 100% saturation to 50% saturation, then to 10% saturation. Fig. 11 systematically shows the dependence of surface coverage of Knot-like and Wheat-like configurations for 2-HA-OC_n (n = 12, 14, 16, 18, 20) on the solution concentration with 1-octanoic acid as the solvent. According to the overall variation tendency, we conclude that Knot-like pattern is preferred when the concentration is decreased to 10% saturation, whereas the Wheat-like structure is favored when the concentration is increased to 100% saturation. It has been widely reported that molecules tend to be arranged in a looser packing fashion under low concentration, while denser packing fashion under high concentration.[1,28,49-51] In addition, the concentration is directly related to the number of solute molecules which get away from the solution and then adsorb on the substrate. Through

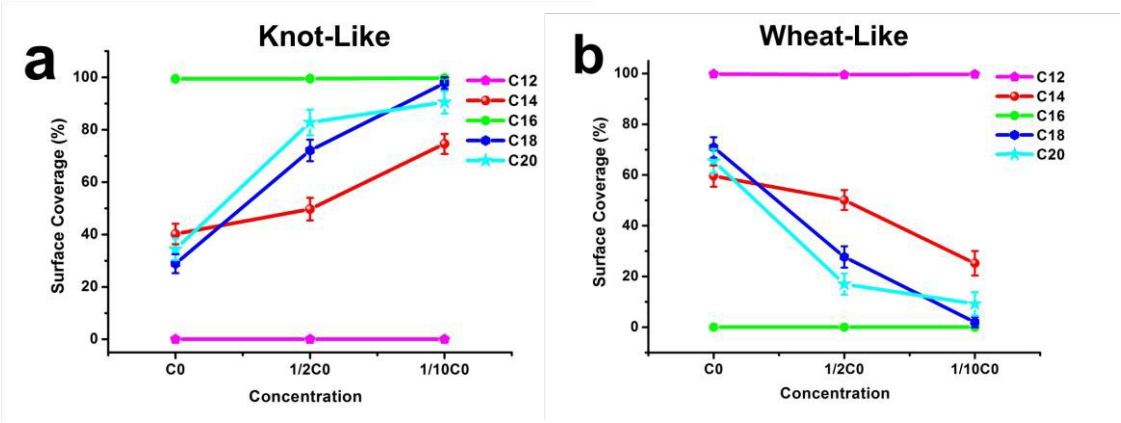

Fig. 11 Dependence of the surface coverage for Knot-like (a) and Wheat-like (b) structures on the concentration. C_0 represents the concentration of 100% saturation (solvent: 1-octanoic acid). The labels refer to 2-HA-OC_n with alkyl chains of different length.

comparing the area density displayed in Table 2, it is clear that the achiral structure of Wheat-like is more closed than the chiral structure of Knot-like. Hence, as the concentration increases, the number of 2-HA-OC_n molecules physisorb onto the graphite surface per time per area increases correspondingly, and as a result, the adsorbates take priority of densely packed Wheat-like pattern. On the contrary, the surface coverage for looser packed Knot-like arrangement increases as the concentration decreases.

4.2.2 Solvent control

In the experimental process of exploring the 2D self-assembly of 2-HA-OC_n molecules, we found that the appearance of the chiral Knot-like and achiral Wheat-like structures is also solvent-dependent. Fig. 8 shows the surface coverage distributions for these two phases in polar solvent of 1-octanoic acid and nonpolar solvent of *n*-tetradecane. From the histograms we draw a conclusion that the looser Knot-like pattern is favored in polar solvent, whereas the denser packed Wheat-like pattern is favored in nonpolar solvent. Beside, even though 1-phenyloctane is classified into nonpolar group, it shows weak polarity.[52] So the polarity of solvents used in the present work has a trend of 1-octanoic acid > 1-phenyloctane > *n*-tetradecane. From the large-scale STM image of 2-HA-OC_{14} molecules self-assembled monolayers on HOPG interface (Fig. 7), we clearly see that as the polarity decreases, the surface coverage for Knot-like pattern decreases, while the surface coverage for Wheat-like pattern increases. Solvent can modulate the self-assembly structures by tuning the type and density of intermolecular interactions[26], or affecting the adsorption energy for solute on the substrate[53]. The dipole induced Knot-like and Wheat-like structures in most cases are coexistent and they differ from each other in their packing density.

In view of the total system energy, closely packed assembly is more frequently favored in which both of the adsorbate−substrate and adsorbate−adsorbate interactions are maximized. However, self-assembly at the liquid/solid interface is more complex. There exists an equilibrium between the adsorption and desorption of the solute molecules. It is speculated that when the solvent−solute interactions are strong, the desolvation energy costs for the solute molecules are high, and as a result, it is relatively hard for the solute to adsorb on the substrate. In contrast, the opposite solvent environment leads to fast and easy formation of the assembled adlayers. The 2-HA-OC_n molecules have polarity, and thus the interaction between solute and high-polar solvent is stronger than that between solute and low-polar or nonpolar solvent. This will affect the adsorption and desorption rate at the solution/solid interface, and then affect the area density. Therefore, in the poor solvent of *n*-tetradecane, the solvophobic effect favors the densely packed achiral Wheat-like structure, whereas in a good solvent of 1-octanoic acid, the solvophilic effect favors the looser packed chiral Knot-like structure.

4.3 Emergence of alkyl chain length effect

The 2D supramolecular structure closely dependent on alkyl chain length has been widely reported to be a common phenomenon.[54-57] Fig. 12 systematically shows the dependence of surface coverage on the length of alkyl chain. Lines in the same color represent the same solvent and concentration, but the solid lines refer to the Knot-like structure and the dotted lines correspond to the Wheat-like pattern.

From the line chart we draw the conclusions from four aspects. 1) When 1-octanoic acid is used as the solvent, no matter how the concentration changes, 2-HA-OC_{16} molecules only self-assemble into Knot-like structure, as indicated by the red, green and orange solid lines. Thus we infer that the Knot-like phase is stable for 2-HA-OC_{16} both kinetically and thermodynamically. 2) When the alkyl chain length is shorter than n = 16, the Knot-like phase gradually change into the Wheat-like phase. The 2-HA-OC_n molecules show polarity and they show strong interaction with the solvent molecules. As the alkyl chain length decreases, the solute−solvent interaction decreases accordingly, thus the number of molecules which desolvate from the solution and then adsorb onto the substrate per time per area increases. Therefore, it is reasonable that the looser Knot-like structure transfers into the denser Wheat-like structure. 3) When the alkyl chain length is longer than n = 16, Wheat-like and Knot-like structures coexist with each other and neither of them shows priority. As we know, the 2D packing fashions on solid surface are controlled by subtle balance among intermolecular, molecule−substrate, and molecule−solvent interactions. The self-assembly process can be affected by even tiny change of these interactions, and as a result, the monolayer

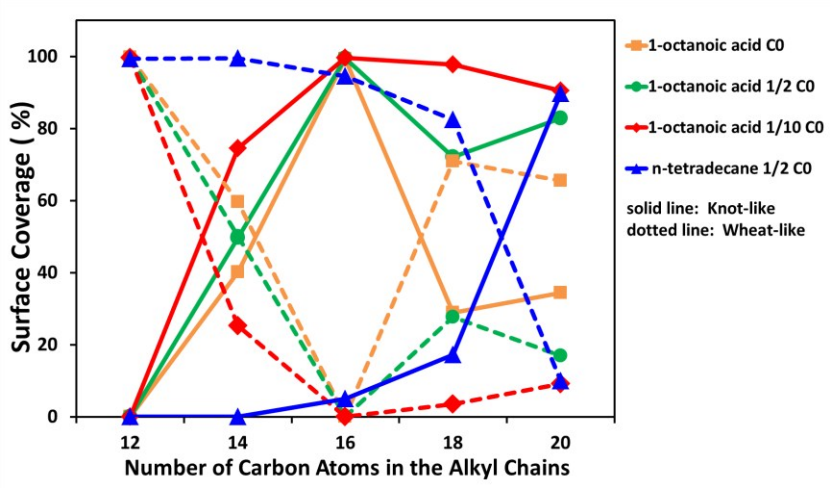

Fig. 12 Surface coverage for Knot-like and Wheat-like structures on the number of carbon atoms in the alkyl chains.

structures are changed. As the alkyl chain length increase, the molecule–solvent interaction increases, and this will decrease the number of solute molecules which physisorb on the substrate surface. However, as the alkyl chain length increases, the molecule–molecule and molecule–substrate interactions increase as well, and then densely-packed Wheat-like arrangement is possibly preferred, thus the two structures are coexistent. 4) When *n*-tetradecane is used as the solvent, the surface coverage show single-changed tendency under the concentration of 50% saturation, as the blue lines (solid and dotted lines) indicated. We have just mentioned that the denser Wheat-like structure is preferred in the nonpolar solvent of *n*-tetradecane (as shown in Fig. 8). This is a general trend, but it is not abnormal that a special case exists because the surface coverage is affected by multiple factors. For example, the surface coverage for the looser Knot-like phase shows a sharp increase when n = 20. This gradually upward tendency can be explained by the gradual increase of molecule–solvent interactions. Moreover, this single-changed tendency is different from the red, green and orange solid lines, which peak at n = 16 and show the cases of using 1-octanoic acid as the solvent. This can be attributed to the difference of the solvent properties. On the whole, the surface coverage for these two structures is controlled by combined factors of solvent effect and concentration effect as the alkyl chain length changes.

4.4 Emergence of odd–even effect

Odd–even effect is a phenomenon which has been thoroughly investigated and widely reported for its influence on molecule crystallization[58], chemical and physical properties[59], and dynamic of monolayers[60,61]. During the systematic STM investigation, we find that the adlayer structures of Wheat-like and Wheat-like´ are affected by odd–even effect. These two configurations differ from each other at the supramolecular level: the relative direction of adjacent V-like ribbons, as shown in Fig. 13, in which 2-HA-OC_{14} and 2-HA-OC_{15} are taken for example. The two adjacent ribbons in Wheat-like phase (Fig. 13a) are opposite in their direction, but in the Wheat-like´ phase (Fig. 13b), the neighboring ribbons in a domain are orienting to the same direction. This difference is attributed to minimum of the steric repulsion. It is generally known that one possible driving force for the alternate bending up and down of the alkyl chains is to have a good match between the alkyl chains and the graphite lattice for the maximization of molecule–substrate interaction.[62] Moreover, to maximize the substrate coverage, which is favored for enthalpic reasons[15], chains in adjacent ribbons are fully interdigitated, giving rise to closely packed configurations and favorable van der Waals interactions between the alkyl chains. In order to get dense 2D packing on surface, carbon atoms of neighboring chains should be staggered with each “up” atom in one chain next to a “down” atom in each of the neighbors.[63] In Fig. 13, the direction of end methyls and the methylenes connected with the ether bonds are denoted by a series of pink arrows. It is clear that the chains in these two packing fashions are well-matched, without repulsive domains. Therefore, whether the two ribbons orient to the same direction or not depends on the relative orientation of the end methyls in the side chains.

Moreover, we have mentioned above that the dipole moment in a domain is extinguished to zero for Wheat-like structure, but

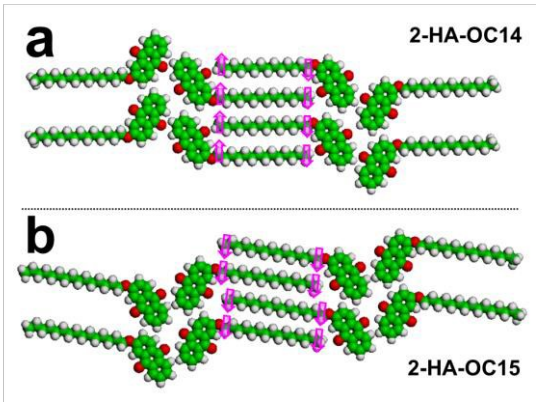

Fig. 13 Space-filling spheres figure representation of the matched end methyls with methylene groups within the interdigitated side chains for Wheat-like structure of 2-HA-OC_{14} (a) and Wheat-like´ structure of 2-HA-OC_{15} (b). The pink arrows indicate the direction of the end carbon atoms.

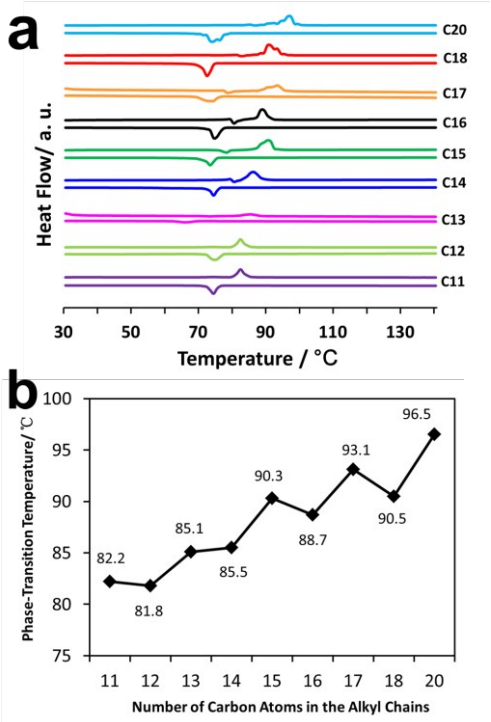

Fig. 14 DSC thermograms of compounds 2-HA-OC_n (*n* = 11−18, 20) for the trace of heating (the above line) and cooling (the below line). (b) Dependence of the phase-transition temperature (melting point) for 2-HA-OC_n derivatives on the number of carbon atoms in the alkyl chains.

isn't for Wheat-like´ structure. Then we infer that this difference may result in alternately changed energy that is needed for 2-HA-OC_n molecules to self-assemble into ordered adlayers. Thereupon, we conducted a series of differential scanning calorimetry (DSC) experiments to explore how odd−even effect can influence the crystallization properties. Fig. 14a is the DSC thermograms, and the peak temperature in the horizontal ordinate is the melting point (phase-transition temperature) of the compounds. It can be evidently seen that as the number of carbon atoms in the side chain increases, the phase-transition temperature of 2-HA-OC_n derivatives increases in an up-down-up-down tendency, as demonstrated by the zigzag line in Fig. 14b. The difference in melting point originates from different energy required to form uniform phase.[64] Then Fig. 14 is a powerful evidence that the energy required for 2-HA-OC_{odd} and 2-HA-OC_{even} to form order arrangements is different in an odd−even way. Thus the odd−even effect on the melting point has a close relationship with the molecular self-assembly patterns.

Conclusion

In summary, we accomplished STM experiments of a series of 2-HA-OC_n (*n* = 12−18, 20) derivatives at the liquid/solid interface. Structural transition between chiral Knot-like and achiral Wheat-like structures which were induced by dipole−dipole and hydrogen bonding interactions could be controlled by changing the concentration and solvent. Molecules tended to arrange in looser Knot-like packing fashion under low concentration, while denser Wheat-like packing fashion under high concentration. This was caused by different number of molecules which desolvate from the solution to adsorb onto the graphite surface per time per area. Besides, as the polarity decreased from 1-octanoic acid to 1-phenyloctane then to *n*-tetradecane, the surface coverage for the chiral Knot-like structure decreased correspondingly, whereas that for Wheat-like structure increased. This variation was attributed to the difference of solvent polarity, which resulted in different solvophobic/solophilic effect, then greatly influenced the molecule−solvent interactions. Odd−even effect was observed in our study. 2-HA-OC_{odd} molecules self-assembled into Wheat-like´ structure, different from the Wheat-like pattern for 2-HA-OC_{even} molecules at supramolecular level. The adjacent V-like ribbons in these two configurations took the same or reverse orientation for the sake of minimizing the steric repulsion. Moreover, the DSC tests were conducted to prove that the energy required for 2-HA-OC_n molecules to form uniform phases changed in an up-down-up-down fashion as the number of carbon atoms in the alkyl chains increased in an odd-even-odd-even tendency. On the whole, dipole−dipole interactions and hydrogen bonds induced chiral and achiral expressions of molecules on achiral surface provide a promising approach for design and fabrication of nanoporous adlayers through controlling the concentration and solvent.

Acknowledgments

Financial supports from the Natural Science Foundation of China (21573077, 21403072, 51373055), the National Program on Key Basic Research Project (2012CB932900), the China Postdoctoral Science Foundation (2014M552189), and the Fundamental Research Funds for the Central Universities (SCUT) are gratefully acknowledged.

Notes and references

1. X. L. Shen, X. D. Wei, P. L. Tan, Y. G. Yu, B. A. Yang, Z. M. Gong, H. M. Zhang, H. P. Lin, Y. Y. Li, Q. Li, Y. S. Xie and L. F. Chi, *Small*, 2015, **11**, 2284−2290.
2. J. Xu, T. Li, Y. F. Geng, D. H. Zhao, K. Deng, Q. D. Zeng and C. Wang, *J. Phys. Chem. C*, 2015, **119**, 9227−9233.
3. H. J. Yan, N. Sandig, H. F. Wang, D. Wang, F. Zerbetto, X. W. Zhan and L. J. Wan, *Chem. Asian J.*, 2015, **10**, 1311−1317.
4. S. Wang, F. Y. Zhao, S. W. Luo, Y. F. Geng, Q. D. Zeng and C. Wang, *Phys. Chem. Chem. Phys.*, 2015, **17**, 12350−12355.
5. K. Tahara, K. Kaneko, K. Katayama, S. Itano, C. H. Nguyen, D. D. D. Amorim, S. De Feyter and Y. Tobe, *Langmuir*, 2015, **31**, 7032−7040.
6. F. P. Cometto, K. Kern and M. Lingenfelder, *ACS Nano*, 2015, **9**, 5544−5550.
7. M. N. Nair, C. Mattioli, M. Cranney, J. P. Malval, F. Vonau, D. Aubel, J. L. Bubendorff, A. Gourdon and L. Simon, *J. Phys. Chem. C*, 2015, **119**, 9334−9341.
8. S. Bonacchi, M. E. Garah, A. Ciesielski, M. Herder, S. Conti, M. Cecchini, S. Hecht and P. Samori, *Angew. Chem. Int. Ed.*, 2015, **54**, 4865−4869.
9. T. Chen, W. H. Yang, D. Wang and L. J. Wan, *Nat. Commun.*, 2013, **4**, 1389−1396.

10. V. Humblot, S. M. Barlow and R. Raval, Prog. *Surf. Sci.*, 2004, **76**, 1–19.
11. R. Raval, *Chem. Soc. Rev.*, 2009, **38**, 707–721.
12. M. Linares, A. Minoia, P. Brocorens, D. Beljonne and R. Lazzaroni, *Chem. Soc. Rev.*, 2009, **38**, 806–816.
13. S. De Feyter, A. Gesquière, M. M. A. Mottaleb, P. C. M. Grim, F. C. De Schryver, C. Meiners, M. Sieffert, S. Valiyaveettil and K. Müllen, *Accounts Chem. Res.*, 2000, **33**, 520–531.
14. N. Katsonis, E. Lacaze and B. L. Feringa, *J. Mater. Chem.*, 2008, **18**, 2065–2073.
15. W. Mamdouh, H. Uji-i, J. S. Ladislaw, A. E. Dulcey, V. Percec, F. C. De Schryver and S. De Feyter, *J. Am. Chem. Soc.*, 2006, **128**, 317–325.
16. L. Xu, X. R. Miao, B. Zha, K. Miao and W. L. Deng, *J. Phys. Chem. C*, 2013, **117**, 12707–12714.
17. R. Gutzler, T. Sirtl, J. F. Dienstmaier, K. Mahata, W. M. Heckl, M. Schmittel and M. Lackinger, *J. Am. Chem. Soc.*, 2010, **132**, 5084–5090.
18. C. Marie, F. Silly, L. Tortech, K. Müllen and D. Fichou, *ACS Nano*, 2010, **4**, 1288–1292.
19. Z. Y. Yang, H. M. Zhang, C. J. Yan, S. S. Li, H. J. Yan, W. G. Song and L. J. Wan, *Proc. Natl. Acad. Sci. U. S. A.*, 2007, **104**, 3707–3712.
20. S. De Feyter, A. Gesquière, M. Klapper, K. Müllen and F. C. De Schryver, *Nano Lett.*, 2003, **3**, 1485–1488.
21. Y. Kikkawa, E. Koyama, S. Tsuzuki, K. Fujiwara, K. Miyake, H. Tokuhisa and M. Kanesato, *Surf. Sci.*, 2007, **601**, 2520–2524.
22. L. Piot, A. Marchenko, J. Wu, K. Müllen and D. Fichou, *J. Am. Chem. Soc.*, 2005, **127**, 16245–16250.
23. L. Kampschulte, M. Lackinger, A. K. Maier, R. S. K. Kishore, S. Griessl, M. Schmittel and W. M. Heckl, *J. Phys. Chem. B*, 2006, **110**, 10829–10836.
24. Y. B. Li, Z. Ma, G. C. Qi, Y. L. Yang, Q. D. Zeng, X. L. Fan, C. Wang and W. Huang, *J. Phys. Chem. C*, 2008, **112**, 8649–8653.
25. X. Shao, X. C. Luo, X. Q. Hu and K. Wu, *J. Phys. Chem. B*, 2006, **110**, 1288–1293.
26. X. Zhang, Q. Chen, G. J. Deng, Q. H. Fan and L. J. Wan, *J. Phys. Chem. C*, 2009, **113**, 16193–16198.
27. L. Xu, X. R. Miao, B. Zha and W. L. Deng, *J. Phys. Chem. C*, 2012, **116**, 16014–16022.
28. C. Meier, M. Roos, D. Künzel, A. Breitruck, H. E. Hoster, K. Landfester, A. Gross, R. J. Behm and U. Ziener, *J. Phys. Chem. C*, 2010, **114**, 1268–1277.
29. N. T. N. Ha, T. G. Gopakumar and M. Hietschold, *J. Phys. Chem. C*, 2011, **115**, 21743–21749.
30. X. R. Miao, L. Xu, L. H. Cui and W. L. Deng, *Phys. Chem. Chem. Phys.*, 2014, **16**, 12544–12553.
31. L. Xu, X. R. Miao, L. H. Cui, P. Liu, X. F. Chen and W. L. Deng, *Nanoscale*, 2015, **7**, 11734–11745.
32. B. Zha, X. R. Miao, P. Liu, Y. M. Wu and W. L. Deng, *Chem. Commun.*, 2014, **50**, 9003–9006.
33. L. Xu, X. R. Miao, L. H. Cui, P. Liu, K. Miao, X. F. Chen and W. L. Deng, *J. Phys. Chem. C*, 2015, **119**, 17920–17929.
34. C. J. Li, Q. D. Zeng, P. Wu, S. L. Xu, C. Wang, Y. H. Qiao, L. J. Wan and C. L. Bai, *J. Phys. Chem. B*, 2002, **106**, 13262–13267.
35. Source: http://www.51pptmoban.com/pic/739.html.
36. Y. Hu, K. Miao, B. Zha, X. R. Miao, L. Xu and W. L.Deng, *RSC Adv.*, 2015, **5**, 93337–93346.
37. L. H. Cui, X. R. Miao, L. Xu, Y. Hu and W. L. Deng, *Phys. Chem. Chem. Phys.*, 2015, **17**, 3627–3636.
38. Y. Kikkawa, E. Koyama, S. Tsuzuki, K. Fujiwara, K. Miyake, H. Tokuhisa and M. Kanesato, *Chem. Commun.*, 2007, 1343–1345.
39. I. Varga, H. Yamada, F. Kun, H. G. Matuttis and N. Ito, *Phys. Rev. E*, 2005, **71**, 051405.
40. Y. Wei, W. Tong, C. Wise, X. Wei, K. Armbrust and M. Zimmt, *J. Am. Chem. Soc.*, 2006, **128**, 13362–13363.
41. D. V. Talapin, E. V. Shevchenko, C. B. Murray, A. V. Titov and P. Král, *Nano Lett.*, 2007, **7**, 1213–1219.
42. X. Y. Wang, T. F. Jiao, Z. X. Zhang, T. Chen, M. H. Liu, L. J. Wan and D. Wang, *J. Phys. Chem. C*, 2013, **117**, 16392–16396.
43. K. S. Mali, K. Lava, K. Binnemans and S. De Feyter, *Chem. Eur. J.*, 2010, **16**, 14447–14458.
44. A. Ciesielski, C. A. Palma, M. Bonini and P. Samori, *Adv Mater*, 2010, **22**, 3506–3520.
45. Z. C. Mu, L. J. Shu, H. Fuchs, M. Mayor and L. F. Chi, *J. Am. Chem. Soc.*, 2008, **130**, 10840–10841.
46. L. J. Wan, *Accounts Chem. Res.*, 2006, **39**, 334–342.
47. T. Yoshinori, M. Kosuke and M. Kazuo, *Bull. Chem. Soc. Jpn.*,2013, **86**, 354–362.
48. S. Lei, K. Tahara, F. C. De Schryver, M. Van der Auweraer, Y. Tobe and S. De Feyter, *Angew. Chem.*, 2008, **120**, 3006–3010.
49. K. Tahara, S. Okuhata, J. Adisoejoso, S. Lei, T. Fujita, S. De Feyter and Y. Tobe, *J. Am. Chem. Soc.*, 2009, **131**, 17583–17590.
50. J. Adisoejoso, K. Tahara, S. Lei, P. Szabelski, W. Rżysko, K. Inukai, M. O. Blunt, Y. Tobe and S. De Feyter, *ACS Nano*, 2012, **6**, 897–903.
51. X. Zhang, T. Chen, Q. Chen, G. J. Deng, Q. H. Fan and L. J. Wan, *Chem. Eur. J.*, 2009, **15**, 9669–9673.
52. J. R. T. Lapasio, M. C. G. A. Coque, M. Roses, E. Bosch, A. M. Zissimos and M. H. Abraham, *Anal. Chim. Acta*, 2004, **515**, 209–227.
53. C. J. Li, Q. D. Zeng, C. Wang, L. J. Wan, S. L. Xu, C. R. Wang and C. L. Bai, *J. Phys. Chem. B*, 2003, **107**, 747–750.
54. X. Shao, X. C. Luo, X. Q. Hu and K. Wu, *J. Phys. Chem. B*, 2006, **110**, 15393–15402.
55. S. Yokoyama, T. Hirose and K. Matsuda, *Chem. Eur. J.*, 2015, **21**, 1–9.
56. K. Tahara, K. Inukai, N. Hara, C. A. Johnson II, M. M. Haley and Y. Tobe, *Chem. Eur. J.*, 2010, **16**, 8319–8328.
57. Y. Miyake, T. Nagata, H. Tanaka, M. Yamazaki, M. Ohta, R. Kokawa and T. Ogawa, *ACS Nano*, 2012, **6**, 3876–3887.
58. M. K. Khan and P. R. Sundararajan, *J. Phys. Chem. B*, 2011, **115**, 8696–8706.
59. G. M. Florio, T. L. Werblowsky, B. Ilan, T. Müller, B. J. Berne and G. W. Flynn, *J. Phys. Chem. C*, 2008, **112**, 18067–18075.
60. F. Tao and S. L. Bernasek, *Chem. Rev.*, 2007, **107**, 1408–1453.
61. Y. Kikkawa, E. Koyama, S. Tsuzuki, K. Fujiwara and M. Kanesato, *Langmuir*, 2010, **26**, 3376–3381.
62. F. Tao and S. L. Bernasek, *Langmuir*, 2007, **23**, 3513–3522.
63. K. G. Nath, O. Ivasenko, J. A. Miwa, H. Dang, J. D. Wuest, A. Nanci, D. F. Perepichka and F. Rosei, *J. Am. Chem. Soc.*, 2006, **128**, 4212–4213.
64. J. Y. Wang, J. Yan, L. Ding, Y. Ma and J. Pei, *Adv. Funct. Mater.*, 2009, **19**, 1746–1752.

Graphical Abstract

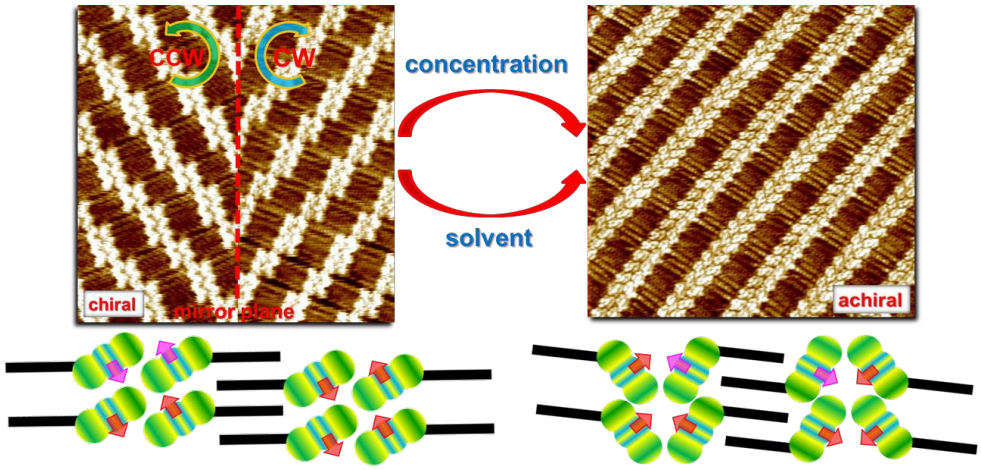

Importance:

The study presents efficient strategies on manipulation of hydrogen bonds and dipole–dipole induced chiral and achiral self-assembly nanostructures.